**4450** *J. Phys. Chem. A* **2006,** *110,* 4450−4457

# Reaction of Cl Atoms with $C_6F_{13}CH_2OH$, $C_6F_{13}CHO$, and $C_3F_7CHO$

**G. Solignac, A. Mellouki,* and G. Le Bras**
*LCSR−CNRS, 1C Avenue de la recherche scientifique, 45071 Orléans Cedex 02, France*

**I. Barnes and Th. Benter**
*Bergische University Wuppertal, Fachbereich C−Physikalische Chemie, Gauss Strasse 20, D-42119 Wuppertal, Germany*

*Received: December 2, 2005; In Final Form: February 1, 2006*

The Cl atom initiated oxidation of $C_6F_{13}CH_2OH$, $C_6F_{13}CHO$, and $C_3F_7CHO$ was investigated at 298 K and 1000 mbar pressure of air in a photoreactor using in situ Fourier transform infrared (FTIR) analysis. The rate coefficient for the reaction Cl + $C_6F_{13}CH_2OH$ (reaction 2) was measured using a relative method: $k_2 = (6.5 \pm 0.8) \times 10^{-13}$ cm$^3$ molecule$^{-1}$ s$^{-1}$. $C_6F_{13}CHO$ was detected as the major primary product, while CO and $CF_2O$ were found to be the major secondary products. A fitting procedure applied to the concentration−time profiles of $C_6F_{13}CHO$ provided a production yield of (1.0 ± 0.2) for this aldehyde in reaction 2, and the rate coefficient for the reaction Cl + $C_6F_{13}CHO$ (reaction 4) was $k_4 = (2.8 \pm 0.7) \times 10^{-12}$ cm$^3$ molecule$^{-1}$ s$^{-1}$. A high CO yield observed in the oxidation of $C_6F_{13}CH_2OH$, (52 ± 1)%, is attributed to the Cl atom initiated oxidation of $C_6F_{13}CHO$. High CO yields, (61 ± 2)% and (85 ± 5)%, were also measured in the Cl atom initiated oxidation of $C_3F_7CHO$ in air and nitrogen, respectively. These high CO yields suggest the occurrence of a decomposition reaction of the perfluoroacyl, $C_6F_{13}CO$, and $C_3F_7CO$ radicals to form CO which will compete with the combination reaction of these radicals with oxygen to form perfluoroacyl peroxy radicals in the presence of air. The latter radicals $C_nF_{2n+1}CO(O)_2$ ($n = 6-12$), through their reaction with $HO_2$ radicals, are currently considered as a possible source of persistent perfluorocarboxylic acids which have been detected in the environment. The consequences of the present results would be a reduction of the strength of this potential source of carboxylic acids in the atmosphere.

## Introduction

Long-chain fluorotelomer alcohols (FTOHs, $C_nF_{2n+1}CH_2CH_2OH$), used in a variety of industrial products, have been suggested as a potential source of persistent perfluorinated carboxylic acids (PFCAs, $C_nF_{2n+1}C(O)OH$, $n = 6-12$) which have been detected in the environment [e.g., ref 1]. PFCAs may be produced in the gas phase from the aldehydes $C_nF_{2n+1}CHO$, which have been shown to be atmospheric oxidation products of FTOHs (e.g., refs 2 and 3 and references therein). Such aldehydes (with $n = 1-4$) have also been established as the sole primary products in the Cl atom initiated oxidation of the fluorinated alcohols $C_nF_{2n+1}CH_2OH$ in air in the absence of NO.[4] Cl atom initiated oxidation is widely used in laboratory experiments to mimic the OH radical initiated oxidation actually occurring in the atmosphere. To contribute to a better knowledge of the atmospheric chemistry of the FTOHs, we have investigated the kinetics and mechanism of the Cl atom initiated oxidation of the 2,2,3,3,4,4,5,5,6,6,7,7,7-tridecafluoro alcohol ($C_6F_{13}CH_2OH$) and of its major observed primary product $C_6F_{13}CHO$. To the best of our knowledge no previous investigation of these reactions has been reported in the literature to date. For comparison the Cl atom initiated oxidation of $C_3F_7CHO$ for which data have already been reported[4,5] has also been investigated.

## Experimental Section

Experiments were performed in a cylindrical 480 L Duran glass reactor (3 m in length, 45 cm in diameter) at 298 ± 2 K and 1000 mbar total pressure of synthetic air. The chamber is described in detail elsewhere.[6] The reactor is surrounded by 20 superactinic lamps (Philips TLA 40W/05, $300 < \lambda < 450$ nm, $\lambda_{max} = 360$ nm) for photolytic initiation of reaction systems. A multireflection White type mirror system (51.6 m optical path length) mounted inside the reactor is interfaced to an Fourier transform infrared (FTIR) spectrometer (Nicolet Magna 520, KBr beam splitter, MCT detector) and allows in situ monitoring of reactants and products in the parts per million range. Chlorine atoms were produced by the photolysis of molecular chlorine:

$$Cl_2 + h\nu \rightarrow Cl + Cl \qquad (1)$$

**Kinetic Studies.** A relative rate method has been used to measure the rate coefficient for the reaction of Cl atoms with $C_6F_{13}CH_2OH$ relative to that of Cl with methyl chloride ($CH_3Cl$):

$$Cl + C_6F_{13}CH_2OH \rightarrow \text{products} \qquad (2)$$

$$Cl + CH_3Cl \rightarrow \text{products} \qquad (3)$$

Provided that the fluoro alcohol and $CH_3Cl$ are consumed only by reaction with Cl atoms, it can be shown that

$$\ln([C_6F_{13}CH_2OH]_0/([C_6F_{13}CH_2OH]_t) = k_2/k_3 \ln([CH_3Cl]_0/([CH_3Cl]_t) \qquad (I)$$

where the subscripts “0” and “*t*” indicate the concentrations of

10.1021/jp0570162 CCC: $33.50

the compounds prior to commencement of the irradiation and at a reaction time *t*, respectively.

Weighed amounts of $C_6F_{13}CH_2OH$ were introduced into the reactor via a heated air stream, while $CH_3Cl$ and $Cl_2$ were introduced by direct injection using calibrated syringes. Initial concentrations of the reactants were in the range of (8.1−8.5) $\times 10^{13}$ molecule $cm^{-3}$ for $C_6F_{13}CH_2OH$, 2.6 $\times 10^{13}$ molecule $cm^{-3}$ for $CH_3Cl$, and 2.6 $\times 10^{13}$ molecules $cm^{-3}$ for $Cl_2$. The concentration−time behaviors of the reactants were monitored using FTIR. Infrared spectra were derived from 64 co-added interferograms recorded with 1 $cm^{-1}$ resolution over 75 s. In typical experiments 10−15 spectra were recorded over a period of 10−20 min. The reactant concentrations were determined with the help of a spectral subtraction procedure using the characteristic IR absorption features of $C_6F_{13}CH_2OH$ and $CH_3Cl$ in the ranges 3550−3650 and 2820−3150 $cm^{-1}$, respectively.

Control experiments were performed in which (i) a $C_6F_{13}CH_2OH/CH_3Cl$/air mixture was irradiated and (ii) a $C_6F_{13}CH_2OH/CH_3Cl$/air/$Cl_2$ mixture was left in the dark for periods exceeding those used in typical experiments (10−20 min). On the time scale of each of these control experiments no significant loss of reactants was observed. These observations support that photolysis and heterogeneous or dark reactions are negligible loss processes for the reactants under the experimental conditions employed.

**Product Studies.** *(i) Cl + $C_6F_{13}CH_2OH$.* A product study of the Cl atom initiated oxidation of $C_6F_{13}CH_2OH$ was performed using the same experimental system and procedure as described above for the kinetic study. Five independent runs were conducted with initial concentrations of $C_6F_{13}CH_2OH$ and $Cl_2$ in the ranges (0.29−1.44) $\times 10^{14}$ and (1−2) $\times 10^{14}$ molecule $cm^{-3}$, respectively. All experiments were conducted in air and in the absence of $NO_x$. The mixtures were irradiated for periods of time ranging between 15 and 120 min and resulted in the extreme case in more than 80% consumption of $C_6F_{13}CH_2OH$.

The IR spectral features used for the analysis of $C_6F_{13}CH_2OH$ were the same as those used for the kinetic study, i.e., 3550−3650 $cm^{-1}$. Again a spectral subtraction procedure was used to derive the concentration of reactants and products as a function of the reaction time. Identification and quantification of the reactants and the reaction products was made using calibrated reference spectra. The calibrated spectra were either produced by introducing known concentrations of authentic samples ($C_6F_{13}CH_2OH$) or were taken from our existing IR spectral library bank (CO and $CF_2O$). Quantification of $C_6F_{13}CHO$, produced in situ in the reactor (see below), was made assuming that the absorption cross section of its C═O stretching band at 1778 $cm^{-1}$ is the same as that of $C_3F_7CHO$ at the same wavenumber. $C_3F_7CHO$ was calibrated assuming the solid introduced into the chamber was 97% $C_3F_7CHO\cdot H_2O$ (commercial purity) and that 100% of the introduced mass was converted into $C_3F_7CHO$ (see Materials section).

*(ii) Cl + $C_3F_7CHO$.* The perfluoroaldehyde $C_3F_7CHO$ was manufactured as described in the Materials section. Product studies of the Cl atom initiated oxidation of $C_6F_{13}CHO$ were performed in a manner similar to that described for the kinetic and product studies on Cl + $C_6F_{13}CH_2OH$. Prior to the product studies control experiments were performed in which (i) a $C_3F_7CHO$/air mixture was irradiated and (ii) a $C_3F_7CHO$/air/$Cl_2$ mixture was left in the dark for periods exceeding those used in typical experiments. On the time scale of each of these control experiments no significant loss of $C_3F_7CHO$ was observed. These observations support that photolysis and heterogeneous or dark reactions are negligible loss processes for $C_3F_7CHO$ under the experimental conditions employed. The initial concentrations for the product studies were (1.1−1.4) $\times 10^{14}$ molecules $cm^{-3}$ for $C_3F_7CHO$ and about 1.6 $\times 10^{14}$ molecule $cm^{-3}$ for $Cl_2$. The mixtures were irradiated using 8−20 lamps for time periods between 8 and 18 min, leading to complete consumption of the aldehyde. For the analysis of $C_3F_7CHO$ the IR spectral feature at (1750−1802) $cm^{-1}$ and integration of the band at (1850−1997) $cm^{-1}$ were used. For the observed products $CF_2O$ and CO, peak height measurements at 976 (baseline 1039−880) $cm^{-1}$ and 1929.5 (baseline 1815−2006) $cm^{-1}$ were used for $CF_2O$ and a peak height measurement at 2119.9 (baseline 2005−2143) $cm^{-1}$ was used for CO (a plot of CO absorbance against CO concentration was linear up to CO concentrations of ∼5 $\times 10^{13}$ molecules $cm^{-3}$).

**Materials.** $C_3F_7CHO$ was obtained from the conversion of the corresponding hydrate ($C_3F_7CH(OH)_2$). Two different methods were used to obtain the desired aldehyde. In the first method, a weighed amount of the commercial hydrate (Matrix Scientific) was introduced via a heated air stream into the chamber without further treatment. This introduction method leads to a mixture of hydrate and aldehyde as shown in Figure 1. A complete conversion of the hydrate to the aldehyde in air was obtained on leaving the mixture to stand in the dark. Figure 1A, trace a, shows the IR spectrum obtained following introduction of the mixture (hydrate/aldehyde) to the chamber, while Figure 1A, trace b, shows the IR spectrum obtained after leaving the mixture in the reactor until complete disappearance of the absorption due to the OH stretch of $C_3F_7CH(OH)_2$ at (3590−3680) $cm^{-1}$. A comparison of both IR spectra with that of a spectrum of $C_3F_7CHO$ reported by Hashikawa et al.[7] (Figure 1A, trace c) clearly shows that the hydrate is completely converted to the aldehyde on standing for a sufficient period. In Figure 2 the IR band intensity of the aldehyde C═O stretch (1746−1793) $cm^{-1}$ is plotted as a function of time and shows that complete conversion is reached after approximately 40 min. After complete conversion into the aldehyde, $C_3F_7CHO$ was left alone in the dark for a further 20 min period and then subjected to irradiation with the lamps, also for 20 min. Wall and photolysis loss of the aldehyde were found to be negligible, and there was also no evidence for any reconversion of the aldehyde to the hydrate.

In the second method, a sample of $C_3F_7CH(OH)_2$ was kept overnight in a glass bulb in 1000 mbar of purified synthetic air and was then introduced into the reactor filled with 200 mbar of synthetic air. The IR spectrum taken immediately after introduction showed that the hydrate had been converted completely to the aldehyde in the glass bulb.

The other reagents were obtained from commercial sources with stated purities of 97% for $C_6F_{13}CH_2OH$ (Fluorochem) and ≥99.8 vol % for $CH_3Cl$ (Messer Griesher) and were used without further purification.

## Results and Discussion

**Rate Coefficient for the Reaction Cl + $C_6F_{13}CH_2OH$.** Two independent runs were performed to derive the rate coefficient for the reaction of Cl atoms with $C_6F_{13}CH_2OH$. Figure 3 shows the kinetic data, for loss of the fluoro alcohol versus $CH_3Cl$, plotted according to eq I. Rate ratios, $k_2/k_3$, of 1.38 $\pm$ 0.7 and 1.35 $\pm$ 0.6 were obtained in the first run and second run, respectively. The rate coefficient for the reaction of Cl with $C_6F_{13}CH_2OH$ has been put on an absolute basis using a value of $k(Cl+CH_3Cl) = 4.8 \times 10^{-13}$ $cm^3$ $molecule^{-1}$ $s^{-1}$ [8] for the reference reaction, which results in values of $k_2 = (6.60 \pm 0.35)$

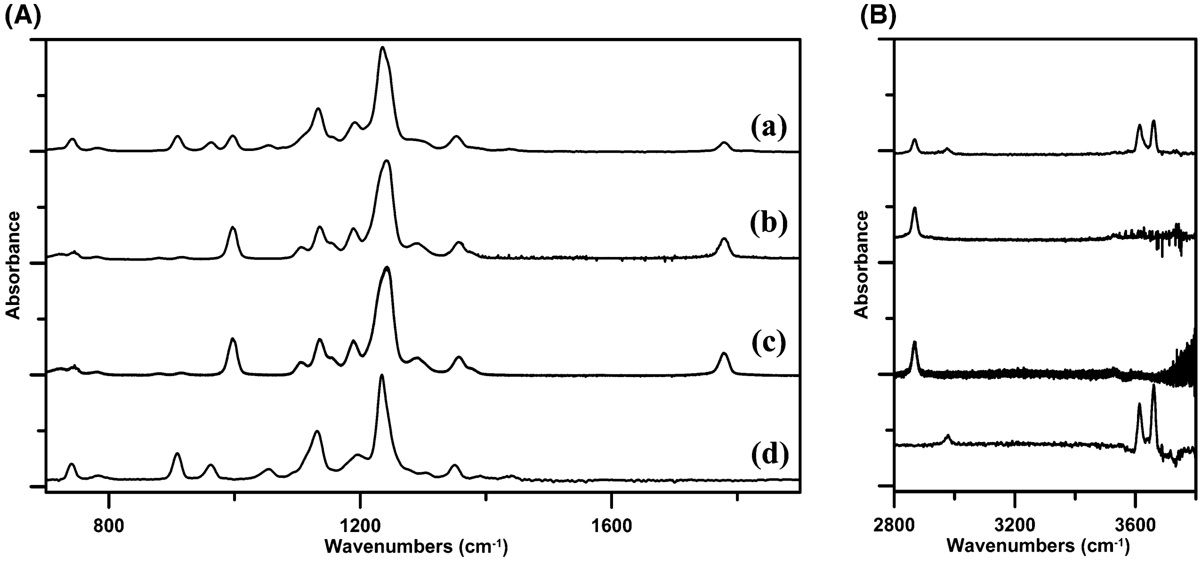

**Figure 1.** (A) Comparison of IR spectra obtained (a) after introduction of the hydrate ($C_3F_7CHO + C_3F_7CHO{\cdot}H_2O$) and (b) after complete conversion into the aldehyde. Trace c is a literature spectrum of $C_3F_7CHO$, and trace d is a spectrum of $C_3F_7CHO{\cdot}H_2O$ obtained after subtraction of (b) from (a). (B) Absorbance (×5) of spectra a−d.

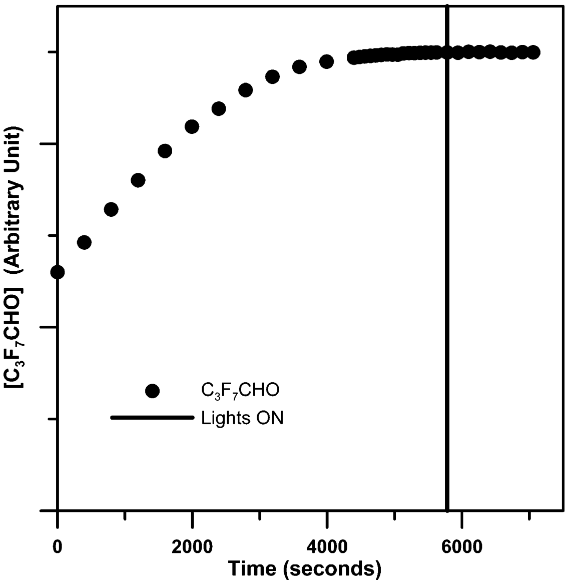

**Figure 2.** Behavior of $C_3F_7CHO$ in the reactor after introduction of the hydrate (lights on for 21 min).

$\times 10^{-13}$ and (6.47 ± 0.15) $\times 10^{-13}$ $cm^3$ $molecule^{-1}$ $s^{-1}$ in the first run and second run, respectively.

The errors quoted are twice the standard deviation arising from the least-squares fits of the data and do not include potential errors associated with uncertainties in the reference rate coefficient. We choose to recommend a final value for $k(Cl+C_6F_{13}CH_2OH)$ of

$$k(Cl+C_6F_{13}CH_2OH) = (6.5 \pm 0.8) \times 10^{-13}\ cm^3\ molecule^{-1}\ s^{-1}$$

which is the average of the values determined in the individual runs. The quoted error includes an estimated 10% uncertainty for the reference rate coefficient.

To our knowledge, this is the first study of the kinetics of the reaction of Cl atoms with $C_6F_{13}CH_2OH$. However, the value obtained in this work can be compared with the rate coefficients reported for the reactions of Cl with shorter chain fluorinated alcohols with the formula $C_nF_{2n+1}CH_2OH$ as listed in Table 1.[4,9,10,11] An examination of the rate coefficients in this table shows very clearly that the length of the $C_nF_{2n+1}$ entity does not have any effect on the reactivity of Cl atoms toward $C_nF_{2n+1}$-$CH_2OH$ since $k(Cl+C_nF_{2n+1}CH_2OH) \approx 6.5 \times 10^{-13}$ $cm^3$ $molecule^{-1}$ $s^{-1}$ for $n = 1-4$ and $n = 6$. This is not surprising since for this compound class the reaction can only proceed via H atom abstraction at the $-CH_2OH$ entity and the first $-CF_2-$ group positioned adjacent to the $-CH_2OH$ group

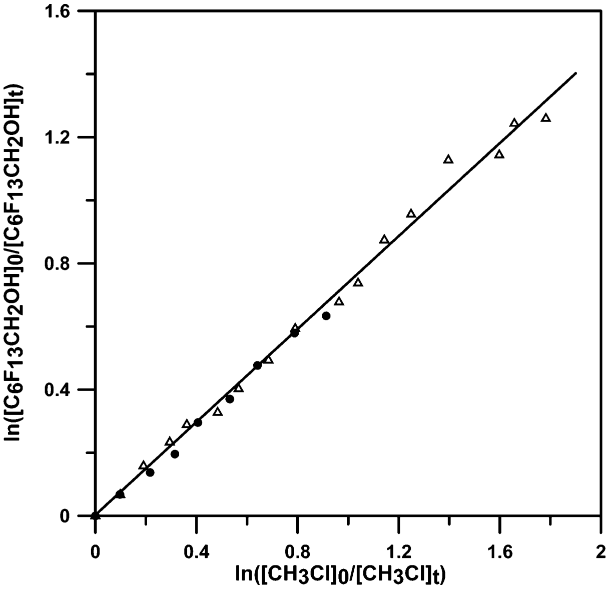

**Figure 3.** Plot of kinetic data according to eq I obtained from two independent experiments on the reaction of Cl with $C_6F_{13}CH_2OH$ measured relative to the reaction of Cl with $CH_3Cl$.

**TABLE 1: Summary of Rate Coefficient Values for Reaction of Cl with $C_nF_{2n+1}CH_2OH$ at Room Temperature**

| fluoro alcohol | $k_{Cl}$ ($cm^3$ $molecule^{-1}$ $s^{-1}$) | reference |
|---|---|---|
| $CF_3CH_2OH$ | (6.3 ± 0.9) $\times 10^{-13}$ | 9 |
| | (7 ± 1) $\times 10^{-13}$ | 10 |
| | (7.42 ± 0.12) $\times 10^{-13}$ | 11 |
| $CF_3CF_2CH_2OH$ | (6.5 ± 0.5) $\times 10^{-13}$ | 4 |
| $CF_3(CF_2)_2CH_2OH$ | (6.5 ± 0.5) $\times 10^{-13}$ | 4 |
| $CF_3(CF_2)_3CH_2OH$ | (6.5 ± 0.5) $\times 10^{-13}$ | 4 |
| $CF_3(CF_2)_5CH_2OH$ | (6.5 ± 0.8) $\times 10^{-13}$ | this work |

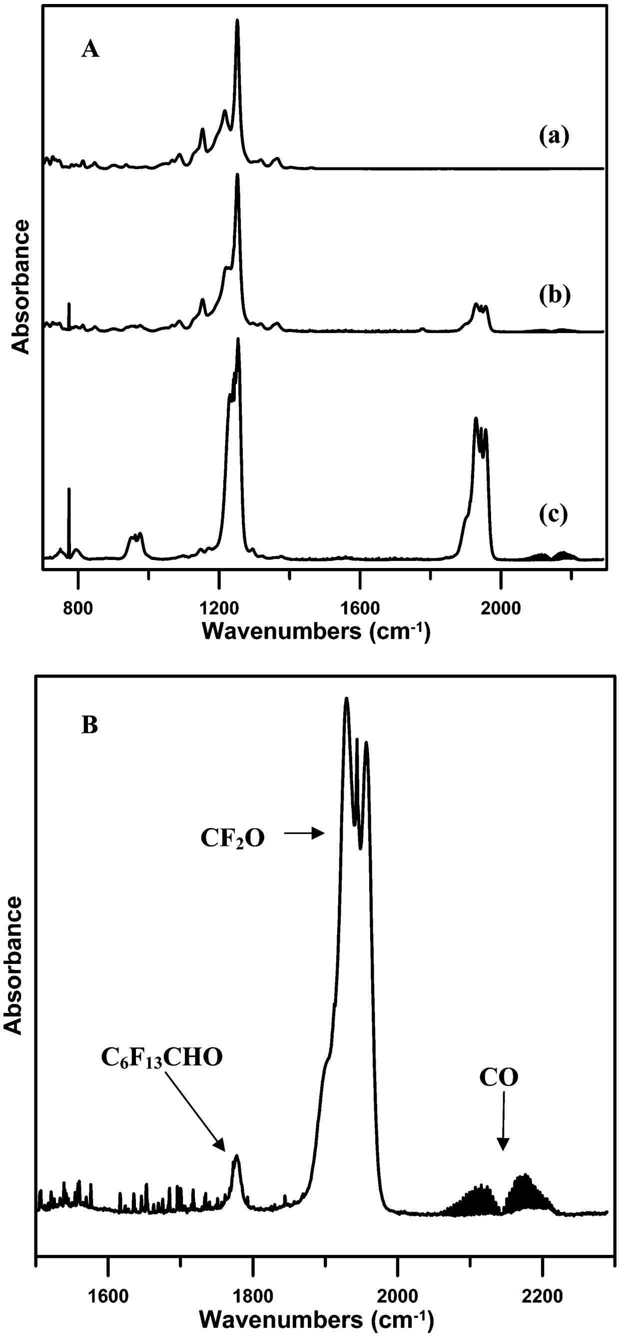

**Figure 4.** (A) Examples of infrared spectra obtained upon irradiation of $C_6F_{13}CH_2OH/Cl_2$/air mixtures used to derive $k(Cl+C_6F_{13}CHO)$. Trace a is a spectrum before irradiation of the mixture, trace b is a spectrum after 8 min irradiation, and trace c is a spectrum after 20 min irradiation, i.e., complete reaction of $C_6F_{13}CHO$ and $C_6F_{13}CH_2OH$. (B) Spectral region 1500−2300 $cm^{-1}$ from trace b showing in detail the identified products CO, $CF_2O$, and $C_6F_{13}CHO$ at a reaction time of 8 min.

already exerts such a strong negative inductive effect on the $-CH_2OH$ group that the addition of further $-CF_2-$ units has a nondiscernible additional influence on the reactivity of the compounds toward Cl.

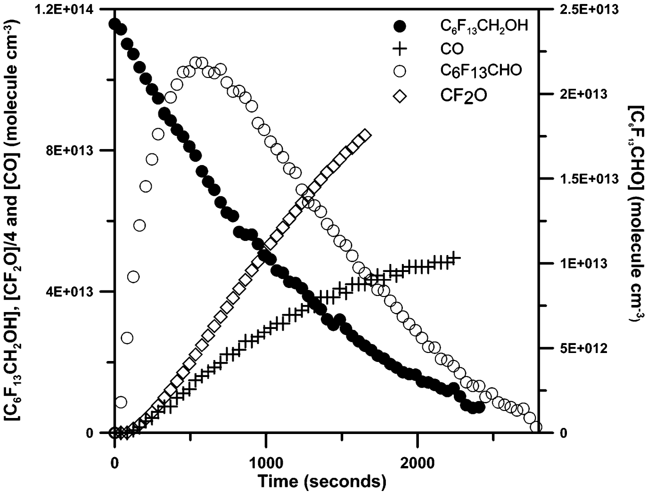

**Figure 5.** Concentration−time profiles of the reactant and main products in the Cl atom initiated oxidation of $C_6F_{13}CH_2OH$ in 1000 mbar of air at 298 K. Note that $[CF_2O]$ is divided by 4.

**Products of the Reaction of Cl with $C_6F_{13}CH_2OH$.** Figure 4A shows typical IR spectra in the spectral range 700−2500 $cm^{-1}$ recorded during investigations on a $C_6F_{13}CH_2OH/Cl_2$/air gas mixture; trace a is a spectrum before irradiation in which the main spectral features are due to $C_6F_{13}CH_2OH$, trace b is a spectrum after 8 min of irradiation, and trace c is a spectrum after complete reaction of $C_6F_{13}CH_2OH$ and $C_6F_{13}CHO$ (approximately 20 min). Figure 4B shows in greater detail the spectral region 1500−2300 $cm^{-1}$ from trace b in Figure 4A in which absorptions due to the identified products CO, $CF_2O$, and $C_6F_{13}CHO$ are clearly evident. The formation of HCl was also observed.

Figure 5 shows an example of the observed concentration−time profiles of $C_6F_{13}CH_2OH$ and the products CO, $CF_2O$, and $C_6F_{13}CHO$. It is clear from Figure 5 that the fluoroaldehyde $C_6F_{13}CHO$ is a primary product of the reaction of Cl with $C_6F_{13}CH_2OH$ and that it is further consumed in the system. The delay in the formation of CO and $CF_2O$ shows that they are being produced in secondary reactions. Carbon monoxide has not been reported as a reaction product in other studies of the OH radical and Cl atom initiated oxidation of fluorinated alcohols $C_nF_{2n+1}CH_2OH$ and fluorinated aldehydes $C_nF_{2n+1}CHO$.[4,5,11]

**Rate Coefficient and Products of the Reaction of Cl with $C_6F_{13}CHO$.** The Cl atom initiated photooxidation of $C_6F_{13}CH_2OH$ with formation of $C_6F_{13}CHO$ can be represented by

$$Cl + C_6F_{13}CH_2OH \rightarrow \alpha C_6F_{13}CHO + HCl \qquad (2')$$

where α represents the production yield of $C_6F_{13}CHO$ from the reaction of Cl with $C_6F_{13}CH_2OH$. Photolysis of the aldehyde under the conditions used in the experiments is negligible; therefore, the observed consumption of the aldehyde in the systems is attributed to reaction with Cl atoms. Reaction of Cl atoms with $C_6F_{13}CHO$ will proceed via an H atom abstraction of the aldehydic hydrogen to produce $C_6F_{13}CO$ radicals.

$$C_6F_{13}CHO + Cl \rightarrow C_6F_{13}CO + HCl \qquad (4)$$

Further reactions of the $C_6F_{13}CO$ radical will lead to the production of other fluorinated compounds, including $CF_2O$, as end products.

To derive a rate coefficient for the reaction of Cl atoms with $C_6F_{13}CHO$, a procedure reported by Meagher et al.[13] and other authors[3,14] has been used. The concentration−time behavior of $C_6F_{13}CHO$ in the experimental system can be represented by the following expression:

$$\frac{[C_6F_{13}CHO]_t}{[C_6F_{13}CH_2OH]_0} = \frac{\alpha(1-x)\{(1-x)^{(k_4/k_2)-1} - 1\}}{\{1-(k_4/k_2)\}} \qquad \text{(II)}$$

where $x = 1 - [C_6F_{13}CH_2OH]_t/[C_6F_{13}CH_2OH]_0$ is the fractional consumption of $C_6F_{13}CH_2OH$ at time $t$, α is the yield of $C_6F_{13}$-

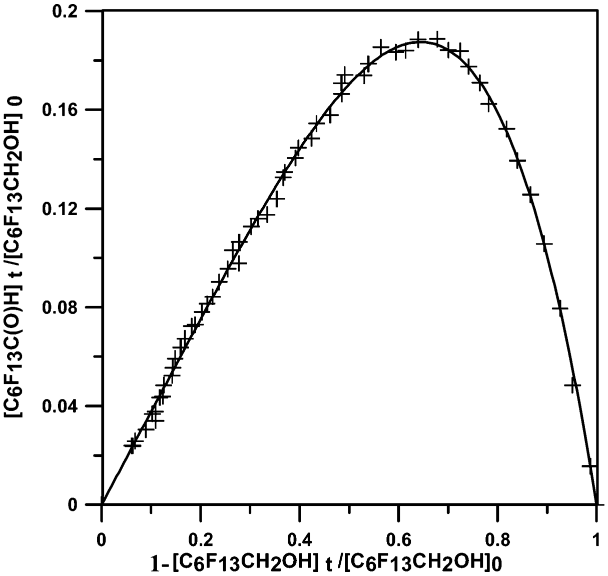

**Figure 6.** Plot of concentration of $C_6F_{13}CHO$ normalized to initial concentration of $C_6F_{13}CH_2OH$ versus fractional loss of $C_6F_{13}CH_2OH$ as observed following irradiation of a $C_6F_{13}CH_2OH/Cl_2$/air mixture. The curve is a fit to eq II.

CHO from the reaction of Cl with $C_6F_{13}CH_2OH$, and $k_4/k_2 = k_{\text{aldehyde}}/k_{\text{alcohol}}$ is the rate coefficient ratio.

Figure 6 shows an example of a plot of the observed $C_6F_{13}CHO$ concentration normalized to the initial concentration of $C_6F_{13}CH_2OH$ versus the fractional loss of $C_6F_{13}CH_2OH$ as a function of irradiation time. The curve is a best fit to the measured points using eq II.

The parameters obtained from five experiments showed very good reproducibility with indistinguishable results within the range of uncertainties.

From the fits an averaged rate coefficient ratio $k_4/k_2$ ($\equiv k_{\text{aldehyde}}/k_{\text{alcohol}}$) of (4.1 ± 1.0) has been obtained. Using a value of $k_2(\text{Cl+C}_6\text{F}_{13}\text{CH}_2\text{OH}) = 6.5 \times 10^{-13}$ cm$^3$ molecule$^{-1}$ s$^{-1}$ leads to a rate coefficient for the reaction of Cl with $C_6F_{13}CHO$ of

$$k_4(\text{Cl+C}_6\text{F}_{13}\text{CHO}) = (2.8 \pm 0.7) \times 10^{-12}\ \text{cm}^3\ \text{molecule}^{-1}\ \text{s}^{-1}$$

The fits give a value of $\alpha = (1.0 \pm 0.2)$ for the production yield of $C_6F_{13}CHO$ in the Cl atom initiated oxidation of $C_6F_{13}CH_2OH$.

The rate coefficient determined here for Cl + $C_6F_{13}CHO$ is compared with those reported in the literature for shorter chain aldehydes ($C_nF_{2n+1}CHO$, $n = 1-4$) in Table 2.[4,5,12,15,16] The reported values would suggest that there is a slight increase in the rate coefficient values on progressing from $CF_3CHO$ ($k = 1.8 \times 10^{-12}$ cm$^3$ molecule$^{-1}$ s$^{-1}$) up to $C_6F_{13}CHO$ ($k = 2.8 \times 10^{-12}$ cm$^3$ molecule$^{-1}$ s$^{-1}$). However, there is substantial overlap of the reported error limits for the rate coefficients of each compound. Sulbaek Andersen et al.[5] have chosen to recommend $k(\text{Cl+C}_n\text{F}_{2n+1}\text{CHO}) = (2.1 \pm 0.5) \times 10^{-12}$ cm$^3$ molecule$^{-1}$ s$^{-1}$ for $n = 1-4$. Taking into account our measurement of $k(\text{Cl+C}_6\text{F}_{13}\text{CHO})$, we suggest a slightly higher value for $k(\text{Cl+C}_n\text{F}_{2n+1}\text{CHO})$ of $(2.5 \pm 1) \times 10^{-12}$ cm$^3$ molecule$^{-1}$ s$^{-1}$ for $n = 1-4$ and $n = 6$ where the error limits encompass the extremes from $CF_3CHO$ to $C_6F_{13}CHO$.

**TABLE 2: Summary of Literature Rate Coefficient Values for Reaction of Cl with $C_nF_{2n+1}CHO$ at Room Temperature**

| $C_nF_{2n+1}CHO$ | $k_{Cl}$ (cm$^3$ molecule$^{-1}$ s$^{-1}$) | technique | reference |
|---|---|---|---|
| $CF_3CHO$ | $(2.7 \pm 0.1) \times 10^{-12}$ | RR[a] | 15 |
| | $(1.8 \pm 0.4) \times 10^{-12}$ | RR[a] | 16 |
| | $(1.9 \pm 0.25) \times 10^{-12}$ | fitting[b] | 4 |
| | $(1.85 \pm 0.26) \times 10^{-12}$ | RR[a] | 5 |
| $C_2F_5CHO$ | $(1.96 \pm 0.28) \times 10^{-12}$ | RR[a] | 12 |
| | $(2.35 \pm 0.42) \times 10^{-12}$ | fitting[b] | 4 |
| $C_3F_7CHO$ | $(2.03 \pm 0.23) \times 10^{-12}$ | RR[a] | 5 |
| | $(2.56 \pm 0.35) \times 10^{-12}$ | fitting[b] | 4 |
| $C_4F_9CHO$ | $(2.34 \pm 0.25) \times 10^{-12}$ | RR[a] | 5 |
| | $(2.48 \pm 0.31) \times 10^{-12}$ | fitting[b] | 4 |
| $C_6F_{13}CHO$ | $(2.8 \pm 0.7) \times 10^{-12}$ | fitting[b] | this work |

[a] Relative rate. [b] Obtained in studies of the reaction of Cl with the corresponding alcohols $C_nF_{2n+1}CH_2OH$.

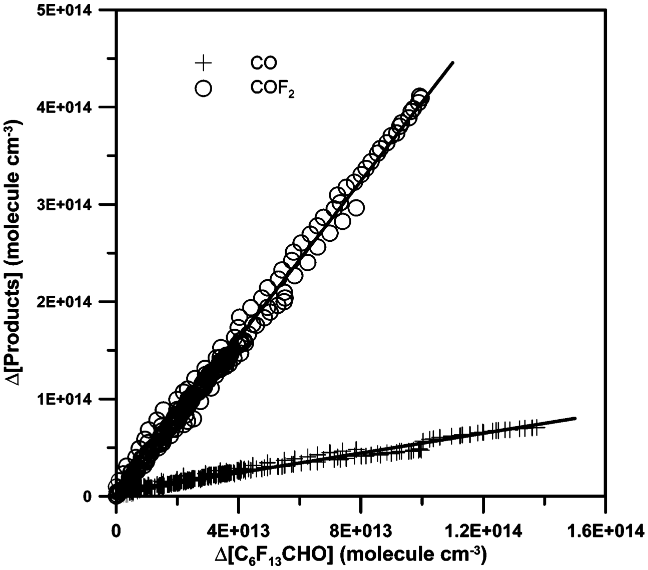

**Figure 7.** Plots of concentrations of CO and $CF_2O$ formed as a function of amount of $C_6F_{13}O$ reacted with Cl atoms for an experiment performed in the absence of $NO_x$ in 1000 mbar of synthetic air at 298 K.

**Products of the Reaction of Cl with $C_6F_{13}CHO$ and with $C_3F_7CHO$.** As discussed above, $CF_2O$ and CO were observed as secondary products in the reaction of Cl with $C_6F_{13}CH_2OH$ in air (Figure 5) and can only be formed in the further oxidation of $C_6F_{13}CHO$. Figure 7 shows a plot of the concentrations of $CF_2O$ and CO formed as a function of the amount of reacted $C_6F_{13}CH_2OH$. Good straight lines were obtained in each case, and molar yields of (404 ± 5)% and (52 ± 1)% have been determined for $CF_2O$ and CO, respectively, in 1000 mbar of air at 298 K.

To establish the source of the products, in particular CO since it has not been reported in other studies, experiments were performed using $C_3F_7CHO$ as a model. Two independent runs were performed in air to investigate the mechanism of the reaction of Cl atoms with $C_3F_7CHO$. Figure 8 shows typical infrared spectra from investigations on a $C_3F_7CHO/Cl_2$/air mixture: Trace a is a spectrum of the mixture before irradiation, trace b is a spectrum after 2 min of irradiation, and trace c is a spectrum recorded after complete reaction of the aldehyde, i.e., approximately 8 min. $CF_2O$ and CO were identified as the major products. In addition, $CF_3OH$ was also identified but could not be quantified since a reference spectrum was not available. The concentration−time profiles of $C_3F_7CHO$, $CF_2O$, and CO from a typical experiment in air are shown in Figure 9. The shapes of the profiles for CO and $CF_2O$ support primary formation routes for both compounds. Figure 10 shows plots of the concentrations of CO and $CF_2O$ versus the consumption of $C_3F_7CHO$ from which production yields of (238 ± 22)% and (61 ± 2)% have been determined for $CF_2O$ and CO, respectively.

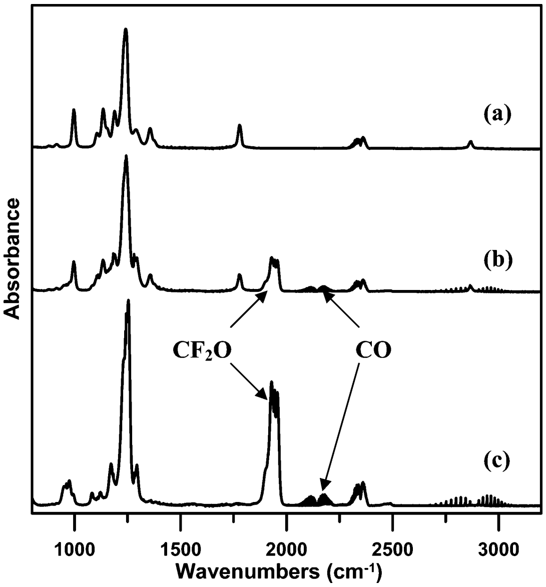

**Figure 8.** IR spectra recorded during experiments on $C_3F_7CHO/Cl_2$/air mixtures: (a) Spectrum of the mixture before irradiation, (b) spectrum after 2 min irradiation, and (c) spectrum after complete reaction of $C_3F_7CHO$ (the $CO_2$ band around 2300−2400 cm$^{-1}$ is due to $CO_2$ in the dry air used to flush the spectrometer).

The reaction of Cl with $C_3F_7CHO$ proceeds by an H atom abstraction of the aldehydic hydrogen to form the $C_3F_7CO$ radical and HCl:

$$Cl + C_3F_7CHO \rightarrow C_3F_7CO + HCl \tag{5}$$

In air the $C_3F_7CO$ radical would be expected to add oxygen to form acylperoxy radicals $C_3F_7C(O)O_2$:

$$C_3F_7CO + O_2 + M \rightarrow C_3F_7C(O)O_2 + M \tag{6}$$

In the atmosphere reactions of these radicals with NO are generally assumed to lead mainly to the formation of $C_3F_7C(O)O$ radicals which rapidly dissociate to form the fluorinated alkyl radical $C_3F_7$ and $CO_2$. In the absence of $NO_x$, as in the present experiments, cross reactions of the peroxy radicals would be expected to lead to the same end result, e.g.

$$C_3F_7C(O)O_2 + C_3F_7C(O)O_2 \rightarrow 2C_3F_7C(O)O + O_2 \tag{7}$$

$$C_3F_7C(O)O + M \rightarrow C_3F_7 + CO_2 + M \tag{8}$$

$C_3F_7$ will react with $O_2$ to form a peroxy radical, and a series of reactions ensues which results in the successive cleavage of $CF_2O$ and ultimately the formation of $CF_3$ radicals. $CF_3$ reacts with $O_2$ to form $CF_3O_2$, which in turn reacts with other peroxy radicals to form $CF_3O$. The $CF_3O$ then reacts with $CF_3O_2$ and hydrogen-containing compounds:

$$CF_3O + CF_3O_2 \rightarrow CF_3O_3CF_3 \tag{9}$$

$$CF_3O + RH \rightarrow CF_3OH + R \tag{10}$$

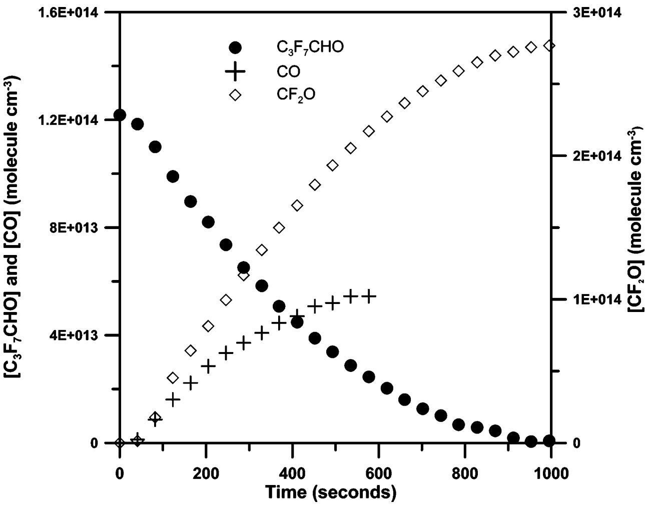

**Figure 9.** Concentration−time profiles of the reactant and main products in the Cl atom initiated oxidation of $C_3F_7CHO$ in 1000 mbar of air at 298 K.

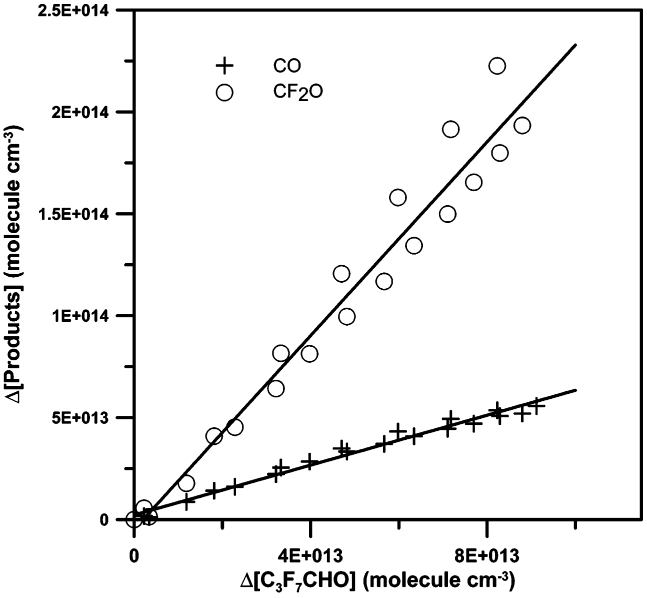

**Figure 10.** Plots of concentrations of CO and $CF_2O$ formed as a function of amount of $C_3F_7CHO$ reacted with Cl atoms for an experiment performed in the absence of $NO_x$ in 1000 mbar of synthetic air at 298 K.

The general mechanism described above is very similar to that reported recently by Sulbaek Andersen et al.[5] for the Cl atom initiated oxidation of $C_nF_{2n+1}CHO$ ($n = 1, 3, 4$). However, this mechanism has no pathway for the formation of CO. As mentioned earlier, CO has not been reported as a product in previous studies on the Cl atom and OH radical initiated oxidation of fluorinated aldehydes and also fluorinated alcohols.[4,5,12] The positive infrared identification in this study of the formation of CO as a primary product in the oxidation of $C_3F_7CHO$ and a secondary product in the oxidation of $C_6F_{13}CH_2OH$ suggests that some common formation pathway is operative. In the case of $C_3F_7CHO$ the most probable pathway is thermal decomposition of the $C_3F_7CO$ radical:

$$C_3F_7CO + M \rightarrow C_3F_7 + CO + M \tag{11}$$

Formation of CO has been observed in the oxidation of other fluorinated compounds. Vésine et al.[17] have observed CO as a secondary product in the Cl and OH initiated oxidation of $C_4F_9CH{=}CH_2$ and $C_6F_{13}CH{=}CH_2$ and proposed the decomposition of $C_4F_9CO$ and $C_6F_{13}CO$ radicals as the probable source.

A series of tests have been performed to ensure that the CO observed in our experiments is really formed during the Cl atom initiated oxidation of the aldehyde in air and is not due to some experimental artifact in our system. Blank runs were performed in which mixtures of molecular chlorine/air and $C_3F_7CHO$/air were photolyzed for a period of time longer than that used during

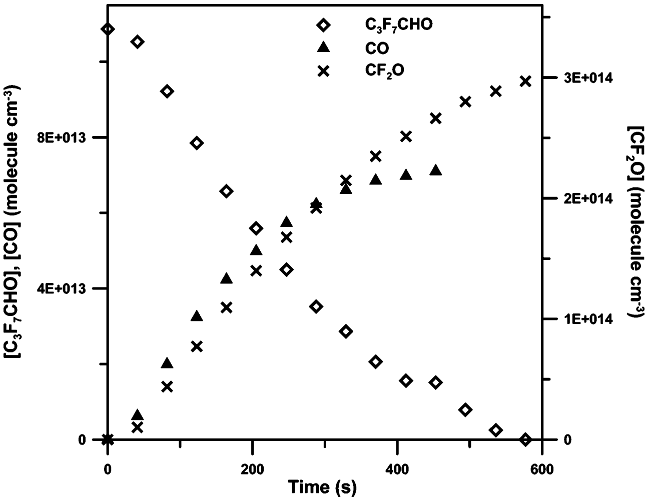

**Figure 11.** Concentration−time profiles of reactants and main products in the Cl atom initiated oxidation of $C_3F_7CHO$ in 1000 mbar of nitrogen at 298 K.

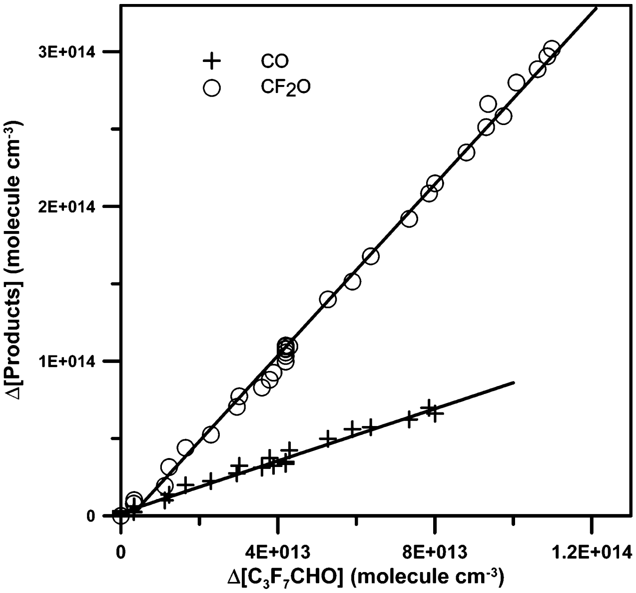

**Figure 12.** Plots of concentrations of CO and $CF_2O$ formed as a function of amount of $C_3F_7CHO$ reacted with Cl atoms for an experiment performed in the absence of $NO_x$ in 1000 mbar of nitrogen at 298 K.

the studies of the reaction of Cl with $C_3F_7CHO$. No quantifiable amount of CO was observed in each case.

If thermal decomposition of $C_3F_7CO$ is the source of CO, then it is occurring in competition with the $O_2$ addition channel which gives $C_3F_7C(O)O_2$. The yield of CO in the oxidation of $C_3F_7CHO$ in air is only 61%; therefore, if the proposed mechanism is valid the yield of CO should show a change upon variation of the $O_2$ partial pressure. To test this, independent runs were performed on $C_3F_7CHO/Cl_2$ mixture in pure nitrogen. In the absence of oxygen the $C_3F_7CO$ radicals formed in the Cl + $C_3F_7CHO$ reaction should decompose to a large extent into CO and $C_3F_7$ radicals due to exclusion of the $O_2$ addition channel. In the absence of $O_2$, some $C_3F_7CO$ might also react with other radicals in the system or $Cl_2$. In the $N_2$ system, CO and $CF_2O$ were observed as products. The concentration−time profiles of $C_3F_7CHO$, $CF_2O$, and CO obtained from irradiation of a $C_3F_7CHO/Cl_2/N_2$ mixture are shown in Figure 11. The concentrations of CO and $CF_2O$ are plotted as a function of consumed $C_3F_7CHO$ in Figure 12. From these plots molar yields of (288 ± 5)% and (85 ± 5)% have been determined for $CF_2O$ and CO, respectively.

Traces of oxygen are always present in the reactor through minor leaks; $O_2$ can be present at concentrations up to 50 ppmv in the worst case, which is enough to oxidize unreactive radicals and explains the observation of $CF_2O$ in $N_2$.

The product data presented here suggest that under ambient conditions ($T$ = 298 K, $P$ = 1000 mbar) there will be competition between the decomposition and $O_2$ addition reaction pathways of the $C_3F_7CO$ and $C_6F_{13}CO$ radicals and that the contribution of the decomposition pathway forming CO is quite significant. This appears to be in contradiction with theoretical calculations on the decomposition rate of $CF_3CO$ that led to the conclusion that only 2% of $CF_3CO$ would decompose under ambient conditions.[18]

## Atmospheric Implications

As mentioned in the Introduction, the persistent PFCAs found in the environment may be produced through reactions of the aldehydes $C_nF_{2n+1}CHO$ which are intermediates in the atmospheric oxidation of FTOHs. The following mechanism has been proposed to explain the formation of PFCAs in the OH radical initiated oxidation of these aldehydes at low $NO_x$ concentrations:

$$C_nF_{2n+1}CHO + OH \rightarrow C_nF_{2n+1}CO + H_2O \qquad (12)$$

$$C_nF_{2n+1}CO + O_2 + M \rightarrow C_nF_{2n+1}C(O)O_2 + M \qquad (13)$$

$$C_nF_{2n+1}C(O)O_2 + HO_2 \rightarrow C_nF_{2n+1}C(O)OH + O_3 \qquad (14)$$

The OH radical initiated oxidation is the only reaction of the aldehydes that has been considered so far for the production of PFCAs. The aldehydes could also possibly photolyze; however, little data exist on their solar photolysis rate and mechanism and it is very likely that photolysis will proceed through C−CHO bond cleavage, producing the $C_nF_{2n+1}O_2$ radical in the presence of air. This radical will not yield the corresponding acid $C_nF_{2n+1}COOH$ (shorter chain PFCAs have also been suggested to be indirectly produced from the $C_nF_{2n+1}O_2$ radical[19]). The branching ratio for the reaction of perfluoroacyl peroxy with $HO_2$ (reaction 4) has been recently determined as 38%, 10%, and 8% for $n$ = 1, 3, and 4, respectively, in 1000 mbar of air at 296 K.[20] In reported mechanisms of perfluoroacyl radicals, such as above, it has always been considered to date that they react entirely with $O_2$ through reaction 13. However, the product data from this work indicate that the decomposition of the perfluroacyl radical can compete quite effectively with reaction 13:

$$C_nF_{2n+1}CO + M \rightarrow C_nF_{2n+1} + CO + M \qquad (15)$$

The CO yield measurements in the Cl atom initiated oxidation of $C_6F_{13}CH_2OH$ and of $C_3F_7CHO$ suggest that around half the $C_nF_{2n+1}CO$ radicals would decompose under ambient conditions. This will reduce by a factor of 2 the yield of PFCAs from FTOHs estimated by considering only reaction 13.

**Acknowledgment.** Financial support from the Telomer Research Programme and the European Science Foundation (ESF) program INTROP is gratefully acknowledged.

## References and Notes

(1) Ellis, D. A.; Martin, J. W.; Mabury, S. A.; Hurley, M. D.; Sulbaek Andersen, M. P.; Wallington, T. *J. Environ. Sci. Technol.* **2003**, *37*, 3816.

(2) Kelly, T.; Bossoutrot, V.; Magneron, I.; Wirtz, K.; Treacy, J.; Mellouki, A.; Sidebottom, H.; Le Bras, G. *J. Phys. Chem. A* **2005**, *109*, 347.

(3) Hurley, M. D.; Misner, J. A.; Ball, J. C.; Wallington, T. J.; Ellis, D. A.; Martin, J. W.; Mabury, S. A.; Sulbeaek Andersen, M. P. *J. Phys. Chem. A* **2005**, *109*, 9816.

(4) Hurley, M. D.; Wallington, T. J.; Sulbaek Andersen, M. P.; Ellis, D. A.; Martin, J. W.; Mabury, S. A. *J. Phys. Chem. A* **2004**, *108*, 1973.

(5) Sulbaek Andersen, M. P.; Nielsen, O. J.; Hurley, M. D.; Ball, J. C.; Wallington, T. J.; Stevens, J. E.; Martin, J. W.; Ellis, D. A.; Mabury, S. A. *J. Phys. Chem. A* **2004**, *108*, 5189.

(6) Barnes, I.; Becker, K. H.; Zhou, T. *Atmos. Environ.* **1973**, *17*, 353.

(7) Hashikawa, Y.; Kawasaki, M.; Waterland, R. L.; Hurley, M. D.; Ball, J. C.; Wallington, T. J.; Sulbaek Andersen, M. P.; Nielsen, O. J. *J. Fluorine Chem.* **2004**, *125*, 1925.

(8) Atkinson, R.; Baulch, D. L.; Cox, R. A.; Hampton, R. F., Jr.; Kerr, J. A.; Rossi, M. J.; Troe, J. *J. Chem. Ref. Data* **1997**, *26*.

(9) Papadimitriou, V. C.; Prosmitis, A. V.; Kambanis, K. G.; Lazarou, Y. G.; Papagiannakopoulos, P. *J. Phys. Chem. A* **2003**, *107*, 3733.

(10) Kelly, T.; Sidebottom, H. Eurotrac Symposium, Garmisch, March 2002 (http://imk-aid afzk.de/CMD/AR 2001/GPP_18_4.pdf).

(11) Sellevag, S. R.; Nielsen, C. J̇.; Søude, O. A.; Myhre, G.; Sundet, J. K.; Stordal, F.; Isaksen, I. S. A. *Atmos. Environ.* **2004**, *38*, 6725.

(12) Sulbaek Andersen, M. P.; Hurley, M. D.; Wallington, T. J.; Ball, J. C.; Martin, J. W.; Ellis, D. A., Mabury, S. A.; Nielsen, O. J. *Chem. Phys. Lett.* **2003**, *379*, 28.

(13) Meagher, R. J.; McIntosh, M. E.; Hurley, M. D.; Wallington, T. J. *Int. J. Chem. Kinet.* **1997**, *29*, 619.

(14) Hurley, M. D.; Ball, J. C.; Wallington, T. J.; Sulbaek Andersen, M. P.; Ellis, D. A.; Martin, J. W.; Mabury, S. A. *J. Phys. Chem. A* **2004**, *108*, 5635.

(15) Scollard, D. J.; Treacy, J. J.; Sidebottom, H.; Ballestra-Garcia, C.; Laverdet, G.; Le Bras, G.; MacLeod, H.; Téton, S. *J. Phys. Chem.* **1993**, *97*, 4683.

(16) Wallington, T. J.; Hurley, M. D. *Int. J. Chem. Kinet.* **1993**, *25*, 819.

(17) Vésine, E.; Bossoutrot, V.; Mellouki, A.; Le Bras, G.; Wenger, J.; Sidebottom, H. *J. Phys. Chem. A* **2000**, *104*, 8512.

(18) Méreau, R.; Rayez, M. T.; Rayez, J. C.; Caralp, F.; Lesclaux, R. *Phys. Chem. Chem. Phys.* **2001**, *3*, 4712.

(19) Ellis, D. A.; Martin, J. W.; De Silva, A. O.; Marbury, S. A.; Hurley, M. D.; Slubaek Andersen, M. P.; Wallington, T. J. *Environ. Sci. Technol.* **2004**, *38*, 3316.

(20) Sulbaek Andersen, M. P.; Stenby, C.; Nielsen, O. J.; Hurley, M. D.; Ball, J. C.; Wallington, T. J.; Martin, J. W.; Ellis, D. A.; Mabury, S. A. *J. Phys. Chem. A* **2004**, *108*, 6325.